



Published in final edited form as:

J Physiol. 2019 September ; 597(17): 4565–4580. doi:10.1113/JP277994.

Liver Sympathetic Denervation Reverses Obesity-Induced Hepatic Steatosis

Chansol Hurr^{1,2}, Hayk Simonyan¹, Donald A. Morgan³, Kamal Rahmouni³, Colin N. Young¹

¹Department of Pharmacology and Physiology, School of Medicine and Health Sciences, The George Washington University, Washington, D.C.

²Department of Physical Education, Chonbuk National University, Jeonju, South Korea

³Department of Pharmacology, University of Iowa, Iowa City, IA.

Abstract

Non-alcoholic fatty liver disease (NAFLD) affects 1 in 3 Americans and is a significant risk factor for type II diabetes mellitus, insulin resistance and hepatic carcinoma. Characterized in part by excessive hepatic triglyceride accumulation (i.e. hepatic steatosis), the incidence of NAFLD is increasing - in line with the growing obesity epidemic. The role of the autonomic nervous system in NAFLD remains unclear. Here, we show that chronic hepatic sympathetic overactivity mediates hepatic steatosis. Direct multiunit recordings of hepatic sympathetic nerve activity were obtained in high fat diet and normal chow fed male C57Bl/6J mice. To reduce hepatic sympathetic nerve activity we utilized two approaches including pharmacological ablation of the sympathetic nerves and phenol-based hepatic sympathetic nerve denervation. Diet-induced NAFLD was associated with a near doubled firing rate of the hepatic sympathetic nerves, which was largely due to an increase in efferent nerve traffic. Furthermore, established high fat diet-induced hepatic steatosis was effectively reduced with pharmacological or phenol-based removal of the hepatic sympathetic nerves, independent of changes in body weight, caloric intake or adiposity. Ablation of liver sympathetic nerves was also associated with improvements in liver triglyceride accumulation pathways including free fatty acid uptake and de novo lipogenesis. These findings highlight an unrecognized pathogenic link between liver sympathetic outflow and hepatic steatosis and suggest that manipulation of the liver sympathetic nerves may represent a novel therapeutic strategy for NAFLD.

Keywords

sympathetic nerve activity; diet-induced obesity; non-alcoholic fatty liver disease; autonomic nervous system

Correspondence: Colin N. Young, Ph.D., 2300 I Street NW, 448 Ross Hall, The George Washington University School of Medicine and Health Sciences, Washington, D.C., 20037, colinyoung@gwu.edu, Phone: 202-994-9575, Fax: 202-994-2870.

Author Contributions

C.H, K.R., and C.N.Y. designed the studies; C.H., H.S., D.M., and C.N.Y. performed and analyzed the experiments; C.H. and C.N.Y. wrote the paper; C.H, H.S., D.M. K.R., and C.N.Y. participated in important discussions of the data and edited the paper. All authors approved the final version of the manuscript.

Competing Interests

None

Introduction

Nonalcoholic fatty liver disease (NAFLD) affects approximately 30% of the US population and is now the primary cause of liver transplants (Angulo, 2002). Directly associated with obesity, startling estimates indicate that approximately 60–75% of obese individuals are affected by NAFLD (Angulo, 2002). NAFLD is a direct result of hepatic steatosis, (Angulo, 2002; Jou *et al.*, 2008), which can progress to non-alcoholic steatohepatitis, cirrhosis, and hepatocellular carcinoma (Jou *et al.*, 2008).

Hepatic lipid accumulation is determined by a complex interplay between de novo lipogenesis, hepatic β -oxidation, free fatty acid (FFA) uptake, and triglyceride disposal from the liver in the form of very low-density lipoprotein (VLDL) (Angulo, 2002; Jou *et al.*, 2008; Vernon *et al.*, 2011). Thus, factors that lead to an imbalance between lipid acquisition (FFA uptake and de novo lipogenesis) and disposal (β -oxidation and VLDL export) can contribute to the development of hepatic steatosis. For example, in rodent models of diet-induced obesity, excess caloric intake has been shown to increase the liver triglyceride pool via unrestrained lipolysis in white adipose tissue (Postic & Girard, 2008), leading to augmented FFA uptake into the liver. In addition, overnutrition-associated mechanisms enhance hepatic de novo lipid synthesis, which is not balanced by parallel elevations in triglyceride disposal through β -oxidation and VLDL export (Lewis *et al.*, 2002).

To date, most studies have taken a “liver-centric” (or adipose tissue) view to delineate cellular and molecular mechanisms contributing to NAFLD (Lewis *et al.*, 2002; Postic & Girard, 2008; Vernon *et al.*, 2011). While essential, it is important to consider that the central nervous system (CNS) is intimately involved in metabolic regulation, with alterations in CNS networks emerging as key culprits in metabolic disease processes (Sandoval *et al.*, 2008; Purkayastha & Cai, 2013). In particular, overactivation of the sympathetic branch of the autonomic nervous system is implicated in a number of pathophysiological conditions that are associated with NAFLD such as hypertension and insulin resistance (Fisher *et al.*, 2009; Grassi *et al.*, 2015). Sympathetic nerve fibers directly innervate and/or lie in close proximity to hepatocytes, Kupfer cells, hepatic stellate cells, and sinusoidal endothelial cells (Lautt, 2009). A limited number of observations implicate sympathetic outflow to the liver in lipid metabolism, VLDL processing, and modulation of glucose metabolism (Carreno & Seelaender, 2004; Dicostanzo *et al.*, 2006; Bruinstroop *et al.*, 2015; Kandilis *et al.*, 2015). However, the extent to which the hepatic sympathetic nervous system is involved in NAFLD is unknown.

Here, we tested the hypothesis that hepatic sympathetic nerve activity (SNA) mediates hepatic steatosis during diet-induced obesity. Our findings reveal profound elevations in sympathetic outflow to the liver in a murine model of high fat diet (HFD)-induced hepatic steatosis. Reducing hepatic SNA with pharmacological or phenol-based methods was sufficient to rescue obesity-induced hepatic steatosis via modulation of liver FFA uptake and de novo lipogenic mechanisms. Collectively, these data demonstrate that hepatic sympathetic overactivity is a key driver of hepatic steatosis during obesity.

Materials and Methods

2. Method Details

a. Study approval—All experimental procedures were approved by the Institutional Animal Care and Use Committees at the George Washington University and the University of Iowa and met the standard guidelines set forth by the National Institutes of Health Guide for the Care and Use of Laboratory Animals.

b. Animals—Male C57BL/6J mice were obtained from Jackson Laboratories or an in-house colony. Mice were provided access to food and water ad libitum and were housed with a 12-hour light-dark cycle. Mice were fed HFD (60% kcal from fat; Research Diets Inc) or normal chow (5% kcal from fat) for a period of 10 weeks starting at 6 weeks of age.

c. Hepatic SNA recordings—Recordings of hepatic SNA were performed as previously described (Tanida *et al.*, 2015b). Mice were first anesthetized (ketamine, 87.5 mg/kg + xylazine, 12.5 mg/kg), and multifiber recordings of hepatic SNA were performed by mounting the hepatic sympathetic nerves on custom-made 36-gauge platinum-iridium recording electrodes (Cooner Wire, Chatsworth, CA). The nerve was fixed to the electrode with silicone gel (World Precision Instruments, Sarasota, FL). Nerve electrodes were attached to a high-impedance probe (Grass instruments, Quincy, MA), amplified with a preamplifier, and filtered (100–1000Hz). The amplified, filtered neural signal was routed through an analogue-digital converter and then to a computer for recording and data analysis. Following recording of overall hepatic SNA (efferent and afferent), the hepatic nerves were sectioned distal to the recording electrodes. In doing so, this allowed for selective recording of efferent nerve traffic, as afferent signals were removed. Hepatic SNA was calculated as a frequency (spikes/s) and integrated voltage (v*s/min), after correcting for postmortem residual noise as previously described (Young *et al.*, 2012; Young *et al.*, 2013; Young *et al.*, 2015).

d. Sympathetic denervation—Two approaches were utilized to reduce SNA as follows:

Pharmacological ablation of sympathetic nerves.: Intraperitoneal injection of 6-hydroxydopamine (6-OHDA; 150 mg/kg, Sigma-Aldrich, St. Louis, MO) or vehicle control (saline) was performed in normal chow and HFD fed mice. 6-OHDA is a well-documented neurotoxin that results in the destruction of catecholaminergic (i.e. sympathetic) nerves when administered peripherally (Cucchiari *et al.*, 1990; Wong *et al.*, 2011; Joers *et al.*, 2014). 6-OHDA or vehicle control was administered once and animals were sacrificed 3 days later.

Phenol-based hepatic sympathetic nerve denervation.: After 10 weeks of HFD (starting at 6 weeks of age) or normal chow feeding, mice were randomly assigned to either liver denervation or sham surgery. Procedures were performed as previously described (Lautt & Carroll, 1984; Cucchiari *et al.*, 1990; Hamada *et al.*, 2007). In brief, mice were anesthetized with ketamine (100 mg/kg) mixed with xylazine (10 mg/kg), and placed on a sterile surgical field. After application of betadine solution, the abdominal cavity was opened with a midline

incision. The hepatic artery, portal vein, and common bile duct were visualized. Using blunt dissection methods, the hepatic artery and portal vein were separated from surrounding tissues including the bile duct. For denervation of the liver sympathetic nerves, a sterile cotton-tipped applicator was soaked in phenol solution (10% phenol in ethyl alcohol) and carefully applied to the surface of the bundle of the hepatic artery and portal vein. The abdominal cavity was washed using 0.9% saline solution to remove excess phenol and minimize adhesion formation. Sham surgeries were performed in an identical manner except that 0.9% saline was used in place of phenol. The viscera abdomen was then closed using internal and external atraumatic sutures, including vicryl 6–0 suture for the muscular layer and silk 6–0 for the cutaneous layer (Ethicon, Somerville, NJ). Postoperative care was provided by subcutaneous injection of ketofen (2.5 mg/kg). Animals were sacrificed one week after the surgery for further analyses.

e. Indirect calorimetry—Body weight, food/water intake, ambulatory activity (laser beam breaks), oxygen consumption (VO_2), and carbon dioxide production (VCO_2) were recorded using a Promethion Metabolic Measurement System (Sable Systems, Las Vegas, NV). Specifically, measurements were obtained over a 24-hour period immediately prior to sacrifice following pharmacological or surgical hepatic denervation as described above. Data were analyzed using custom macros in ExpeData software (Sable Systems).

f. Liver histology and immunohistochemistry

Histology: For hematoxylin and eosin (H&E) staining, fresh livers were obtained upon sacrifice and immediately placed in 10% formalin overnight. The tissue was paraffin embedded and then sectioned at 5 μm . Standard H&E staining procedures were performed by the George Washington University School of Medicine and Health Sciences Pathology Core. For staining of neutral lipids, standard Oil Red O procedures were followed (Mehlem *et al.*, 2013). Briefly, fresh liver tissue was dehydrated in 30% sucrose solution for 1 hour and then quickly frozen in a dry ice/isopropanol bath. Tissues were subsequently embedded in OCT fixation medium. Frozen liver tissue was cryosectioned at 14 μm and equilibrated in 60% isopropyl alcohol for 5 min. Liver sections were then incubated in filtered Oil Red O solution (Alfa Aesar, Haverhill, MA) for 7 min and washed with running tap water for 10 min. Water-soluble medium (Vector Laboratories, Burlingame, CA) was used for coverslip mounting. Images were obtained using a light microscopy (Olympus BX43, Center Valley, PA).

Immunohistochemistry—Liver sample preparation and sectioning was performed similar to the procedures described for Oil Red O staining above, except 16 μm sections were used. Liver sections were dried at room temperature and then equilibrated in PBS solution for 20 min. Sections were blocked with 0.3% BSA solution in PBS and incubated with anti-CD36 (1:200, Novus Biologicals, Littleton, CO) overnight. They were then washed three times with PBS for 10 min and subsequently incubated with a goat anti-rabbit antibody (1:1000, Abcam, Cambridge, MA), which was followed by 3 consecutive 10 min PBS washes. Sections were then dried at room temperature and counterstained with DAPI mounting medium (Vector Laboratories, Burlingame, CA). Images were obtained using a light microscopy (Olympus BX43, Center Valley, PA).

g. Quantitative real time PCR—Total RNA was isolated from the liver by Trizol (Invitrogen, Carlsbad, CA) extraction. In brief, liver samples were homogenized, and the resulting homogenized mixture was separated using a chloroform solution. The supernatant was removed, and RNA was precipitated using sodium acetate and isopropanol. The RNA pellet was purified using a series of ethanol washes and the pellet was dissolved in RNase free water. RNA was converted to cDNA using a commercially available kit (Quanta Bioscience, Beverly, MA). cDNA samples of 25 ng were subjected in duplicate to real-time quantitative PCR (Bio-Rad, Hercules, CA). For each target gene, the average expressed isoform was expressed relative to a housekeeping gene (18s) and the relative fold change was calculated using the comparative Ct method (Livak & Schmittgen, 2001). Primer sequences were derived from *Mus musculus* (National Center for Biotechnology Information GenBank).

h. Western blot—Liver tissue (50–100 µg) was washed with PBS, and homogenized in a 1 mL mixture of lysis buffer EDTA and protease inhibitor cocktail (Thermo Scientific, Waltham, MA) with a 6:1 ratio, followed by 30 min incubation on ice. Homogenized samples were centrifuged for 15 min at 14,000 g at 4 °C. The supernatant was then collected while avoiding the lipid layer and insoluble cellular debris. Protein concentration was determined using a BCA protein quantification kit (Thermo Scientific, Waltham, MA). For Western blotting, 10 µg of protein extracts was reduced, denatured, and separated on 4–12% Bis-Tris gels (Invitrogen, Carlsbad, CA). Sample proteins were transferred onto polyvinylidene fluoride membranes, which were then blocked in blocking reagent (Invitrogen, Carlsbad, CA) for 30 min. Membranes were incubated with primary antibodies with respective secondary antibodies for 4 hours. Immunoblots were incubated with a luminol-based chemiluminescent substrate (Thermo Scientific, Waltham, MA) for 5 min and imaged with a digital blot scanner (LI-COR, Lincoln, NE). The signal intensity of each band was normalized to that of the loading control GAPDH in the same membrane.

i. Liver triglyceride measurements—Livers were frozen on dry ice and stored at –80°C. Hepatic triglycerides were extracted, and quantified using a triglyceride colorimetric assay kit (Biovision, Milpitas, CA) according to the manufacturer's protocol. Briefly, liver tissue (~50 mg) was homogenized in 5% Triton X-100 solution, followed by heating in a water bath at 90°C for 5 min. After cooling to room temperature, insoluble cellular components were removed by microcentrifugation for 2 min. The supernatant of the liver tissue was combined with a triglyceride probe, enzyme mix and lipase (all supplied by the manufacturer) and absorbance was measured at 570 nm in a microtiter plate reader (BioTek, Winooski, VT). Blank and lipase controls (i.e. samples without lipase) were subtracted from the optical density of each sample to allow for the quantification of triglycerides. The concentrations were interpolated from the linear regression, and normalized by wet liver weight. All measurements were replicated in duplicate.

j. Tissue norepinephrine measurement—Fresh frozen liver, kidney, pancreas, and spleen (25~50 mg) were homogenized in a 1 mL mixture of hydrogen chloride (10 mM) in the presence of EDTA (1 mM) and sodium metabisulfite (4 mM). After 4°C centrifugation for 20 min at 13,000g, sample supernatants were obtained and used for a standard BCA

assay for protein quantification (Thermo Scientific, Waltham, MA). The sample supernatants were then used for a quantitative determination of norepinephrine using a commercially available competitive ELISA kit (LDN, Nordhorn, Germany). Absorbance was measured at 450 nm in a plate reader (BioTek, Winooski, VT), and tissue norepinephrine concentrations were interpolated from a spline standard curve and normalized by the total protein concentration. All measurements were replicated in duplicate. Values (Table 1) are presented as an absolute and relative to the respective control group to account for variability between different ELISA kits/plates.

k. Quantification and Statistical Analysis—Data are expressed as mean \pm SEM. Multiple group comparisons were evaluated using two-way ANOVA followed by Tukey's post-hoc analysis. Student's two-tailed unpaired t-tests were used for comparisons between two groups. Significance was set at $p < 0.05$.

Results

Dietary-induced NAFLD is associated with robust elevations in hepatic SNA

Given the emerging role of the sympathetic nervous system in metabolic diseases (e.g. Fisher *et al.*, 2009), we first determined if obesity is associated with changes in sympathetic outflow to the liver. Direct multiunit nerve recordings of hepatic SNA were obtained in male C57Bl/6J mice following 10-weeks of HFD or normal chow feeding. A near doubling of hepatic SNA was found in diet-induced obese animals (Figure 1A & 1B), relative to normal chow controls, and was evident when quantified both as a frequency and integrated voltage of the nerve signal (Figure 1B). This increase in hepatic SNA appeared to be partially due to efferent nerve traffic, as elevated nerve activity remained after sectioning the nerve distal to the recording site (i.e. removal of afferent input; Figure 1C & 1D). These findings indicate that obesity-induced NAFLD is characterized by a state of hepatic sympathetic overactivity.

Chemical denervation reduces obesity-induced hepatic steatosis

Based on the findings in Figure 1, we reasoned that hepatic sympathetic overactivity may be a key contributor to diet-induced hepatic steatosis. Normal chow and HFD fed mice were given a single administration of the neurotoxin 6-OHDA (i.p.) to ablate the sympathetic nerves (Cucchiari *et al.*, 1990; Wong *et al.*, 2011), or vehicle control, and sacrificed 3 days later. When administered peripherally, 6-OHDA has been shown to destroy sympathetic nerves without influencing brain noradrenergic or dopaminergic neurons (Kostrzewa & Jacobowitz, 1974). In line with our direct hepatic SNA recordings (Figure 1), liver protein expression of tyrosine hydroxylase, the rate-limiting enzyme for catecholamine synthesis within postganglionic nerve terminals [i.e. a marker of sympathetic innervation (Long & Segal, 2009)], was elevated in control obese mice, relative to normal chow counterparts (Figure 2A). Three days following 6-OHDA administration reductions in liver tyrosine hydroxylase expression in obese mice were evident (Figure 4A), which was further validated with liver norepinephrine measurements (Table 1).

As expected, diet-induced obesity elicited elevations in liver weight and triglycerides (Figure 2B-C). Interestingly, ablation of sympathetic nerves with 6-OHDA reduced the HFD-

mediated hepatomegaly and hepatic steatosis (Figure 2B-C). This was further confirmed at a histological level, with H&E staining revealing extensive lipid accumulation in HFD mice, while liver appearance returned back towards normal chow levels following sympathetic ablation (Figure 2D). In addition to steatosis, NAFLD is associated with alterations in hepatic gluconeogenesis and lipid production/handling. Consistent with prior reports (Hurtado del Pozo *et al.*, 2011; Souza Pauli *et al.*, 2014), mRNA expression of key gluconeogenic [glucose-6-phosphatase (*G6Pase*) and phosphoenolpyruvate carboxykinase (*PEPCK*)] and lipid metabolism [carbohydrate response element binding protein (*ChREBP*) and peroxisome proliferator-activated receptor alpha (*Ppara*)] markers were increased in the liver of diet-induced obese mice relative to normal chow controls (Figure 2E). Three days following 6-OHDA-induced sympathetic denervation, these transcript levels were significantly reduced in HFD fed mice (Figure 2E). Together, these findings demonstrate that short-term pharmacological ablation of sympathetic nerves partially rescues obesity-induced liver steatosis with associated alterations in key glucose and lipid metabolism pathways in the liver.

6-OHDA-induced removal of SNA did not alter body mass, caloric intake, water consumption, locomotor activity, and adipose tissue mass in HFD or normal chow mice (Figure 3A-E). Twenty-four hour indirect calorimetry evaluations indicated that HFD vehicle treated mice preferentially utilized fat as an energy source when compared with lean controls (i.e. respiratory exchanged ratio; RER, Figure 3H). Greater fat utilization was evident in obese mice following removal of SNA (Figure 3H), although whether this is due to a direct liver effect or changes in other metabolic tissues is unclear due to the systemic administration of 6-OHDA. Whole body oxygen consumption (VO_2), carbon dioxide production (VCO_2), and energy expenditure were not influenced by 3-day ablation of sympathetic nerves in either diet group (Figure 3F-G and I). Collectively, these data indicate that while short-term ablation of peripheral sympathetic nerves reduces hepatic steatosis (Figure 2C-D), this is not due to changes in body mass, food intake, locomotor activity, energy expenditure, or adiposity.

Phenol-based hepatic sympathetic denervation improves HFD-induced hepatic steatosis

Next, we performed selective sympathetic denervation of the liver, as previously described (10% phenol application, see Methods) (Lautt & Carroll, 1984; Cucchiari *et al.*, 1990). In line with our direct hepatic SNA recordings (Figure 1), liver protein expression of tyrosine hydroxylase, the rate-limiting enzyme for catecholamine synthesis within postganglionic nerve terminals [i.e. a marker of sympathetic innervation (Long & Segal, 2009)], was robustly elevated in sham operated obese mice, relative to normal chow counterparts (Figure 4A). One-week following hepatic sympathetic denervation, reductions in liver tyrosine hydroxylase expression in obese mice confirmed the efficacy of this approach (Figure 4A), which was further validated with liver norepinephrine measurements (Table 1). Importantly, norepinephrine content was not altered in organs that are also innervated by the mesenteric and celiac ganglia including the pancreas, spleen, and kidney (Table 1).

We subsequently assessed whether selective removal of the liver sympathetic nerves influenced obesity-induced hepatic steatosis. Although liver weight was comparable

between sham and hepatic denervated groups (Figure 4B), removal of sympathetic nerves to the liver in obese mice resulted in a rapid reduction in HFD-induced hepatic steatosis within one week (Figure 4C). Oil Red O staining of neutral lipids and H&E histological evaluation confirmed abrogation of HFD-induced hepatic steatosis and lipid vacuole accumulation following hepatic denervation (Figure 4D-E). Hepatic triglyceride levels were comparable between sham and denervated mice that were fed normal chow (Figure 4C-E). These striking findings are in line with chemical removal of the sympathetic nerves (i.e. 6-OHDA) and highlight a novel role for the hepatic sympathetic nervous system in obesity-induced hepatic steatosis.

While HFD feeding resulted in increased body mass, relative to normal chow, this was not altered in normal chow or HFD groups one week after selective liver denervation (Figure 4E). Similarly, caloric intake, water consumption, and locomotor activity were not influenced by hepatic denervation (Figure 4F-H). As anticipated, subcutaneous inguinal and visceral gonadal white adipose tissue, as well as interscapular brown adipose tissue masses were significantly increased following HFD (Figure 5A); liver denervation did not change the weight of these adipose tissues. Similarly, the weight of neighboring organs that share the same sympathetic ganglia, including the pancreas, spleen, and kidney, were not altered by hepatic denervation (Figure 5A). HFD-associated changes in VO_2 , VCO_2 , substrate partitioning (i.e. RER), and energy expenditure were also not influenced by liver sympathetic denervation (Figure 5B-E). Together, these findings indicate a robust effect of hepatic SNA on liver triglyceride accumulation during diet-induced obesity, which occurs independent of body weight, food/water intake, activity, or adiposity.

Hepatic sympathetic nerve ablation during diet-induced hepatic steatosis affects liver lipid acquisition pathways

To investigate the underlying mechanisms through which removal of hepatic SNA decreases obesity-induced steatosis, we evaluated pathways of hepatic lipid acquisition and disposal. An abnormal FFA uptake into highly oxidative tissues including the liver has been linked to numerous obesity-associated metabolic diseases (Chiu *et al.*, 2005; Doege *et al.*, 2006; Wu *et al.*, 2006). Previous findings indicate that ~60% of hepatic triglycerides are derived from plasma non-esterified FFAs (Donnelly *et al.*, 2005), which are taken up by hepatocyte cell membrane transporters, including cluster of differentiation 36 (CD36) (Coburn *et al.*, 2000) and fatty acid transport proteins (FATP) (Doege *et al.*, 2006). Liver homogenates from obese NAFLD animals demonstrated robust elevations in *CD36* and *FATP5* (liver-specific FATP isoform) transcript levels (Figure 6A), which is consistent with previous findings in humans and rodents (Koonen *et al.*, 2007; Mitsuyoshi *et al.*, 2009; Miquilena-Colina *et al.*, 2011) and suggestive of increased hepatic FFA uptake during NAFLD. Immunohistochemistry confirmed widespread diet-induced elevations in hepatic CD36 (Figure 6C). *Ppara* expression, which is involved, in part, in the regulation of FFA uptake in response to elevated FFAs (Schoonjans *et al.*, 1997), was also elevated in the liver of obese mice when compared with normal chow controls (Figure 6A). One week following hepatic denervation, liver FFA transporter and *Ppara* expression was attenuated in HFD fed animals, indicative of reduced FFA uptake in response to removal of hepatic sympathetic outflow (Figures 6A and C). These findings are intriguing in light of previous work demonstrating that up- and/or

down-regulation of FATP5 and CD36 (Koonen *et al.*, 2007; Doege *et al.*, 2008; Wilson *et al.*, 2016), worsens and/or attenuates hepatic steatosis, respectively. Moreover, they suggest that hepatic sympathetic overactivity may contribute to NAFLD by enhancing liver FFA uptake.

Liver triglycerides are also synthesized from glucose via de novo lipogenesis, with this pathway contributing to ~25% of the total hepatic triglyceride pool in NAFLD individuals (Donnelly *et al.*, 2005; Lambert *et al.*, 2014). Expression levels of hepatic *G6Pase*, as well as the glucose-responsive transcription factor *ChREBP*, were elevated following HFD feeding and subsequently reduced one week following removal of the liver sympathetic nerves (Figure 6B). Hepatic mRNA levels of sterol regulatory element binding protein 1c (*SREBP1c*), an insulin-responsive transcription factor involved in lipogenic gene regulation, were elevated in obese mice, but not influenced by liver sympathetic denervation (Figure 6B). Additional analysis indicated marked HFD-induced elevations in hepatic acyl-CoA:diacylglycerol acyltransferase (DGAT) 1 and 2; enzymes that catalyze the final step in triglyceride synthesis through covalent joining of fatty acyl CoA with diacylglycerol. In this context, liver specific overexpression of DGAT results in hepatic steatosis, independent of insulin resistance (Monetti *et al.*, 2007). Hepatic denervation restored *DGAT1* and *DGAT2* levels in obese mice back to normal chow levels (Figure 6D). Overall, these findings demonstrate that removal of the hepatic sympathetic nerves during diet-induced NAFLD reduces markers of de novo lipogenesis.

The steady state balance of liver triglycerides is also determined by consumption of fatty acids via β -oxidation, as well as export in the form of VLDL. Western blot evaluation of hepatic carnitine palmitoyltransferase 1a (CPT1a), as an indirect indicator of mitochondrial β -oxidation, and acyl-coenzyme A oxidase 1 (ACOX1), as a marker of peroxisomal β -oxidation, were significantly elevated in HFD mice (Figure 6E-F). Liver denervation did not influence CPT1 and ACOX1 (Figure 6E-F) in either diet group, suggesting minimal influence of the liver sympathetic nerves on β -oxidation - at least in the short-term. Similarly, removal of the liver sympathetic nerves did not alter hepatic expression of microsomal triglyceride transfer protein (MTTP), an endoplasmic reticulum protein involved in the processing of VLDL particles (Figure 6G).

Discussion

We report here that hepatic SNA has a direct role in mediating hepatic steatosis during obesity. First, in the context of obesity-induced NAFLD, our data demonstrate a striking elevation in liver SNA that is mediated, at least in part, by increases in efferent sympathetic outflow. Moreover, we provide direct evidence that liver SNA is functionally linked to NAFLD, as pharmacological or phenol-based removal of the liver sympathetic nerves was sufficient to reduce hepatic steatosis during HFD feeding. Short-term removal of the liver sympathetic nerves appeared to beneficially alter hepatic triglyceride storage by influencing lipid acquisition pathways, with less of an effect on triglyceride disposal mechanisms. Collectively, these findings identify a novel and previously unrecognized role for hepatic sympathetic outflow in the pathogenesis of NAFLD.

Sympathetic outflow is critical for modulating physiological processes (Loewy & Spyer, 1990; Dampney, 1994). However, exaggerated elevations in SNA can lead to changes in the function of peripheral end organs (Fisher *et al.*, 2009; Hurr & Young, 2016). For example, obesity-induced cardiovascular diseases (e.g. hypertension) have been suggested to be mediated, in part, by elevations in SNA to renal and vascular beds, whereas emerging evidence suggests a metabolic disease role for the sympathetic nervous system (Fisher *et al.*, 2009; Purkayastha *et al.*, 2011a; Purkayastha *et al.*, 2011b; Hurr & Young, 2016). However, it is important to consider that there is vast heterogeneity in the outflow and responsiveness of efferent sympathetic nerve traffic, and it is now clear that SNA is differentially regulated in an organ specific manner (Osborn & Kuroki, 2012; Hurr & Young, 2016). In this context, the current findings provide the first demonstration that established obesity is associated with profound elevations in liver SNA. The large contribution of efferent nerve traffic further suggests that this obesity-associated hepatic sympathetic overactivity is driven by CNS mechanisms versus alterations in afferent sensing (although direct recordings of afferent SNA are warranted to definitively address this). Central control of sympathetic outflow is determined by a complex interplay between circulating factors that act upon the brain, afferent inputs, and integration of neural signals from higher order autonomic CNS networks (Loewy & Spyer, 1990; Dampney, 1994). While less investigated relative to other sympathetic nerves, an emerging body of literature has begun to provide insight into the CNS control of liver SNA. For example, acute elevations in the hormone leptin result in large increases in liver SNA (Tanida *et al.*, 2015b); findings that are intriguing given that leptin is chronically elevated in obese conditions. Additional evidence points to hypothalamic regions (paraventricular nucleus of the hypothalamus and arcuate nucleus) as key brain sites involved in the control of liver sympathetic outflow, with involvement from the phosphatidylinositol 3-kinase, extracellular signal-regulated kinase 1/2, and melanocortin signaling pathways (Tanida *et al.*, 2011; Tanida *et al.*, 2015a; Tanida *et al.*, 2015b). Thus, the current results provide a framework for future investigations to determine whether alterations in the aforementioned mechanisms, as well as additional neural circuits, molecular pathways, and metabolic factors, contribute to liver sympathetic overactivity during NAFLD.

Pharmacological and phenol-based removal of liver SNA further demonstrated that hepatic sympathetic overactivity is not a by-product of obesity, but is functionally linked to hepatic steatosis during HFD feeding. The reduction in HFD-mediated liver triglyceride accumulation following removal of the liver sympathetic nerves occurred independent of changes in whole body energy expenditure, adiposity, food intake and locomotor activity, supporting a hepatic specific effect. Importantly, we cannot exclude an influence of 6-OHDA on other metabolic organs. Slight differences in the two methodological approaches were noted, with an approximate 50% and 30% reduction in hepatic steatosis with 6-OHDA and phenol-based denervation, respectively. The precise reason for these differences remains unclear, although the greater reduction with 6-OHDA is likely due to the systemic ablation of sympathetic nerves. For example, 6-OHDA will also result in the removal of sympathetic innervation of adipose tissue, which in turn would presumably reduce adipose tissue lipolysis and the availability of circulating FFA's available for the liver. Furthermore, and strikingly, the reduction in obesity-associated hepatic steatosis was very rapid following both

6-OHDA (3 days) and phenol (7 days) denervation. This not only highlights the plastic nature of the liver, but also may be a reflection of the diet-induced model. The HFD murine model (at least with 10 weeks of feeding) represents as a scenario of steatosis without significant liver injury. In line with this, our recent findings using 3-day pharmacological manipulations of the CNS also demonstrated a rapid resolution of hepatic steatosis in HFD fed mice (Horwath *et al.*, 2017). Although comparisons in timecourse between rodents and humans is difficult, clinical literature also suggests that hepatic steatosis can be rapidly resolved within 1 month in humans (Choudhary *et al.*, 2015).

As mentioned above, NAFLD pathogenesis can arise from disruption in the normal mechanisms for transport, synthesis, and removal of fatty acids and triglycerides. In this context, numerous hormonal and nutritional factors have been linked to altered hepatic lipid homeostasis (Angulo, 2002; Jou *et al.*, 2008). Our findings extend this work by not only demonstrating that NAFLD is neurogenically mediated, but also that liver sympathetic outflow appears to promote steatosis through a selective effect on triglyceride accrual versus catabolic pathways. Importantly, hepatic steatosis was not completely rescued in obese animals by 6-OHDA or selective liver denervation. While this may be a reflection of the acute protocols employed (3 and 7 days following denervation), it also not surprisingly indicates that HFD-induced hepatic steatosis is induced by a combination of sympathetic and non-sympathetic mechanisms. Whether liver SNA works in concert with and/or independent from other NAFLD mediators is unclear. For example, insulin resistance and NAFLD are closely associated, with hyperglycemia and hyperinsulinemia promoting hepatic steatosis (Schwarz *et al.*, 2003). Interestingly, we found reductions in glucose (*ChREBP*) and insulin (*SREBP1c*) regulated transcription factors, suggesting a parallel steatotic influence of hepatic SNA and insulin resistance. Moreover, sympathetic overactivity has been suggested to lead to insulin resistance (Purkayastha *et al.*, 2011b). Thus, it is plausible that excessive elevations in efferent hepatic sympathetic outflow could promote hepatic steatosis independently or interactively with known NAFLD mechanisms. However, in-depth future investigations into liver specific and whole-body metabolic parameters, such as glucose handling and insulin sensitivity, are warranted in this regard.

While NAFLD is commonly seen in obese or overweight individuals, NAFLD has also been observed in lean humans (i.e. lean NAFLD). For example, previous reports indicate that the prevalence of NAFLD in lean South Korea populations was 13% (Kwon *et al.*, 2012), whereas 75% of NAFLD-diagnosed patients in rural India had a body mass index lower than 25 kg/m² (Das *et al.*, 2010). However, the exact mechanisms of lean NAFLD remain still unclear. Although speculative, the current findings suggest that liver sympathetic overactivity may play a potential role in the pathophysiology of NAFLD in lean individuals. In addition, the underlying factors that contribute to the progression of hepatic steatosis to further liver injury including non-alcoholic steatohepatitis and cirrhosis remain incompletely defined. Although findings are limited, intriguingly, systemic α -adrenoceptor antagonism or 6-OHDA treatment has been shown to reduce liver injury in a murine model of non-alcoholic steatohepatitis induced by a methionine choline diet (Oben *et al.*, 2003). Together with the findings of the present study, this raises the possibility that, in addition to contributing to liver steatosis, hepatic SNA may also play a role in the progression to steatohepatitis.

Of note, Bruinstroop and colleagues found no change in hepatic steatosis 6 weeks following surgical removal of the hepatic sympathetic nerves in obese Zucker rats (Bruinstroop *et al.*, 2015). While the discrepancy between this previous work and the current results are unclear, consideration of the experimental obesity model is warranted. As mentioned above, leptin acting within the CNS increases hepatic SNA (Tanida *et al.*, 2015b); the obese Zucker rat harbors a missense mutation in the leptin receptor and therefore, whether this genetic model of obesity (versus diet-induced) exhibits elevations in sympathetic outflow to the liver is unclear. Indeed, it is possible that hepatic SNA plays a role in certain forms of obesity-induced hepatic steatosis, but not others. It is also important to consider that the phenol-based approach will also result in removal of parasympathetic nerves, and therefore, we cannot rule a contribution of the parasympathetic branch to our findings. However, given that we found similar effects (i.e. reduction in steatosis) with 6-OHDA and phenol-based denervation, combined with clear elevations in directly recorded hepatic SNA following HFD feeding, the current findings point to hepatic sympathetic outflow a key contributor to hepatic steatosis.

Overall, these findings highlight a novel role for the liver sympathetic nervous system in hepatic steatosis, and suggest that manipulation of the hepatic sympathetic nerves may represent a novel therapeutic approach for NAFLD.

Acknowledgements

The authors thank Melanie L. Judice for her technical assistance.

Funding

NIH R00116776, NIH P01HL084207 and R01DK117007

References

- Angulo P (2002). Nonalcoholic fatty liver disease. *The New England journal of medicine* 346, 1221–1231. [PubMed: 11961152]
- Bruinstroop E, Eliveld J, Foppen E, Busker S, Ackermans MT, Fliers E & Kalsbeek A. (2015). Hepatic denervation and dyslipidemia in obese Zucker (fa/fa) rats. *Int J Obes (Lond)* 39, 1655–1658. [PubMed: 26134416]
- Carreno FR & Seelaender MC. (2004). Liver denervation affects hepatocyte mitochondrial fatty acid transport capacity. *Cell Biochem Funct* 22, 9–17. [PubMed: 14695648]
- Chiu HC, Kovacs A, Blanton RM, Han X, Courtois M, Weinheimer CJ, Yamada KA, Brunet S, Xu H, Nerbonne JM, Welch MJ, Fettig NM, Sharp TL, Sambandam N, Olson KM, Ory DS & Schaffer JE. (2005). Transgenic expression of fatty acid transport protein 1 in the heart causes lipotoxic cardiomyopathy. *Circulation research* 96, 225–233. [PubMed: 15618539]
- Choudhary NS, Saraf N, Saigal S, Gautam D, Lipi L, Rastogi A, Goja S, Menon PB, Bhangu P, Ramchandra SK, Soin AS. (2015). Rapid reversal of hepatic steatosis with life style modifications in highly motivated liver donors. *J Clin Exp Hepatol* 5, 123–126. [PubMed: 26155039]
- Coburn CT, Knapp FF Jr., Febbraio M, Beets AL, Silverstein RL & Abumrad NA. (2000). Defective uptake and utilization of long chain fatty acids in muscle and adipose tissues of CD36 knockout mice. *The Journal of biological chemistry* 275, 32523–32529. [PubMed: 10913136]
- Cucchiari G, Yamaguchi Y, Mills E, Kuhn CM, Anthony DC, Branum GD, Epstein R & Meyers WC. (1990). Evaluation of selective liver denervation methods. *The American journal of physiology* 259, G781–785. [PubMed: 2240220]

- Dampney RA. (1994). Functional organization of central pathways regulating the cardiovascular system. *Physiological reviews* 74, 323–364. [PubMed: 8171117]
- Das K, Das K, Mukherjee PS, Ghosh A, Ghosh S, Mridha AR, Dhobar T, Bhattacharya B, Bhattacharya D, Manna B, Dhali GK, Santra A & Chowdhury A. (2010). Nonobese population in a developing country has a high prevalence of nonalcoholic fatty liver and significant liver disease. *Hepatology* 51, 1593–1602. [PubMed: 20222092]
- Dicostanzo CA, Dardevet DP, Neal DW, Lautz M, Allen E, Snead W & Cherrington AD. (2006). Role of the hepatic sympathetic nerves in the regulation of net hepatic glucose uptake and the mediation of the portal glucose signal. *American journal of physiology Endocrinology and metabolism* 290, E9–E16. [PubMed: 16105863]
- Doerge H, Baillie RA, Ortegon AM, Tsang B, Wu Q, Punreddy S, Hirsch D, Watson N, Gimeno RE & Stahl A. (2006). Targeted deletion of FATP5 reveals multiple functions in liver metabolism: alterations in hepatic lipid homeostasis. *Gastroenterology* 130, 1245–1258. [PubMed: 16618416]
- Doerge H, Grimm D, Falcon A, Tsang B, Storm TA, Xu H, Ortegon AM, Kazantzis M, Kay MA & Stahl A. (2008). Silencing of hepatic fatty acid transporter protein 5 in vivo reverses diet-induced non-alcoholic fatty liver disease and improves hyperglycemia. *The Journal of biological chemistry* 283, 22186–22192. [PubMed: 18524776]
- Donnelly KL, Smith CI, Schwarzenberg SJ, Jessurun J, Boldt MD & Parks EJ. (2005). Sources of fatty acids stored in liver and secreted via lipoproteins in patients with nonalcoholic fatty liver disease. *The Journal of clinical investigation* 115, 1343–1351. [PubMed: 15864352]
- Fisher JP, Young CN & Fadel PJ. (2009). Central sympathetic overactivity: maladies and mechanisms. *Auton Neurosci* 148, 5–15. [PubMed: 19268634]
- Grassi G, Mark A & Esler M. (2015). The sympathetic nervous system alterations in human hypertension. *Circulation research* 116, 976–990. [PubMed: 25767284]
- Hamada T, Eguchi S, Yanaga K, Inuo H, Yamanouchi K, Kamohara Y, Okudaira S, Tajima Y & Kanematsu T. (2007). The effect of denervation on liver regeneration in partially hepatectomized rats. *J Surg Res* 142, 170–174. [PubMed: 17574578]
- Horwath JA, Hurr C, Butler SD, Guruju M, Cassell MD, Mark AL, Davisson RL, Young CN. (2017). Obesity-induced hepatic steatosis is mediated by endoplasmic reticulum stress in the subfornical organ of the brain. *JCI Insight* 2(8), 90170. [PubMed: 28422749]
- Hurr C & Young CN. (2016). Neural Control of Non-vasomotor Organs in Hypertension. *Curr Hypertens Rep* 18, 30. [PubMed: 26957306]
- Hurtado del Pozo C, Vesperinas-Garcia G, Rubio MA, Corripio-Sanchez R, Torres-Garcia AJ, Obregon MJ & Calvo RM. (2011). ChREBP expression in the liver, adipose tissue and differentiated preadipocytes in human obesity. *Biochimica et biophysica acta* 1811, 1194–1200. [PubMed: 21840420]
- Joers V, Dilley K, Rahman S, Jones C, Shultz J, Simmons H & Emborg ME. (2014). Cardiac sympathetic denervation in 6-OHDA-treated nonhuman primates. *PLoS One* 9, e104850. [PubMed: 25133405]
- Jou J, Choi SS & Diehl AM. (2008). Mechanisms of disease progression in nonalcoholic fatty liver disease. *Semin Liver Dis* 28, 370–379. [PubMed: 18956293]
- Kandilis AN, Papadopoulou IP, Koskinas J, Sotiropoulos G & Tiniakos DG. (2015). Liver innervation and hepatic function: new insights. *J Surg Res* 194, 511–519. [PubMed: 25555404]
- Koonen DP, Jacobs RL, Febbraio M, Young ME, Soltys CL, Ong H, Vance DE & Dyck JR. (2007). Increased hepatic CD36 expression contributes to dyslipidemia associated with diet-induced obesity. *Diabetes* 56, 2863–2871. [PubMed: 17728375]
- Kostrzewa RM & Jacobowitz DM. (1974). Pharmacological actions of 6-hydroxydopamine. *Pharmacological reviews* 26, 199–288. [PubMed: 4376244]
- Kwon YM, Oh SW, Hwang SS, Lee C, Kwon H & Chung GE. (2012). Association of nonalcoholic fatty liver disease with components of metabolic syndrome according to body mass index in Korean adults. *Am J Gastroenterol* 107, 1852–1858. [PubMed: 23032980]
- Lambert JE, Ramos-Roman MA, Browning JD & Parks EJ. (2014). Increased de novo lipogenesis is a distinct characteristic of individuals with nonalcoholic fatty liver disease. *Gastroenterology* 146, 726–735. [PubMed: 24316260]

- Lautt WW. (2009). In *Hepatic Circulation: Physiology and Pathophysiology* San Rafael (CA).
- Lautt WW & Carroll AM. (1984). Evaluation of topical phenol as a means of producing autonomic denervation of the liver. *Canadian journal of physiology and pharmacology* 62, 849–853. [PubMed: 6498614]
- Lewis GF, Carpentier A, Adeli K & Giacca A. (2002). Disordered fat storage and mobilization in the pathogenesis of insulin resistance and type 2 diabetes. *Endocr Rev* 23, 201–229. [PubMed: 11943743]
- Livak KJ & Schmittgen TD. (2001). Analysis of relative gene expression data using real-time quantitative PCR and the 2⁻(Delta Delta C(T)) Method. *Methods* 25, 402–408. [PubMed: 11846609]
- Loewy AD & Spyer KM. (1990). *Central autonomic pathways* Oxford University Press New York, 88–103.
- Long JB & Segal SS. (2009). Quantifying perivascular sympathetic innervation: regional differences in male C57BL/6 mice at 3 and 20 months. *J Neurosci Methods* 184, 124–128. [PubMed: 19651158]
- Mehlem A, Hagberg CE, Muhl L, Eriksson U & Falkevall A. (2013). Imaging of neutral lipids by oil red O for analyzing the metabolic status in health and disease. *Nat Protoc* 8, 1149–1154. [PubMed: 23702831]
- Miquilena-Colina ME, Lima-Cabello E, Sanchez-Campos S, Garcia-Mediavilla MV, Fernandez-Bermejo M, Lozano-Rodriguez T, Vargas-Castrillon J, Buque X, Ochoa B, Aspichueta P, Gonzalez-Gallego J & Garcia-Monzon C. (2011). Hepatic fatty acid translocase CD36 upregulation is associated with insulin resistance, hyperinsulinaemia and increased steatosis in non-alcoholic steatohepatitis and chronic hepatitis C. *Gut* 60, 1394–1402. [PubMed: 21270117]
- Mitsuyoshi H, Yasui K, Harano Y, Endo M, Tsuji K, Minami M, Itoh Y, Okanoue T & Yoshikawa T. (2009). Analysis of hepatic genes involved in the metabolism of fatty acids and iron in nonalcoholic fatty liver disease. *Hepatol Res* 39, 366–373. [PubMed: 19054139]
- Monetti M, Levin MC, Watt MJ, Sajjan MP, Marmor S, Hubbard BK, Stevens RD, Bain JR, Newgard CB, Farese RV Sr., Hevener AL & Farese RV Jr. (2007). Dissociation of hepatic steatosis and insulin resistance in mice overexpressing DGAT in the liver. *Cell Metab* 6, 69–78. [PubMed: 17618857]
- Oben JA, Roskams T, Yang S, Lin H, Sinelli N, Li Z, Torbenson M, Huang J, Guarino P, Kafrouni M & Diehl AM. (2003). Sympathetic nervous system inhibition increases hepatic progenitors and reduces liver injury. *Hepatology* 38, 664–673. [PubMed: 12939593]
- Osborn JW & Kuroki MT. (2012). Sympathetic signatures of cardiovascular disease: a blueprint for development of targeted sympathetic ablation therapies. *Hypertension* 59, 545–547. [PubMed: 22311900]
- Postic C & Girard J. (2008). Contribution of de novo fatty acid synthesis to hepatic steatosis and insulin resistance: lessons from genetically engineered mice. *The Journal of clinical investigation* 118, 829–838. [PubMed: 18317565]
- Purkayastha S & Cai D. (2013). Neuroinflammatory basis of metabolic syndrome. *Mol Metab* 2, 356–363. [PubMed: 24327952]
- Purkayastha S, Zhang G & Cai D. (2011a). Uncoupling the mechanisms of obesity and hypertension by targeting hypothalamic IKK-beta and NF-kappaB. *Nat Med* 17, 883–887. [PubMed: 21642978]
- Purkayastha S, Zhang H, Zhang G, Ahmed Z, Wang Y & Cai D. (2011b). Neural dysregulation of peripheral insulin action and blood pressure by brain endoplasmic reticulum stress. *Proceedings of the National Academy of Sciences of the United States of America* 108, 2939–2944. [PubMed: 21282643]
- Sandoval D, Cota D & Seeley RJ. (2008). The integrative role of CNS fuel-sensing mechanisms in energy balance and glucose regulation. *Annu Rev Physiol* 70, 513–535. [PubMed: 17988209]
- Schoonjans K, Martin G, Staels B & Auwerx J. (1997). Peroxisome proliferator-activated receptors, orphans with ligands and functions. *Curr Opin Lipidol* 8, 159–166. [PubMed: 9211064]
- Schwarz JM, Linfoot P, Dare D & Aghajanian K. (2003). Hepatic de novo lipogenesis in normoinsulinemic and hyperinsulinemic subjects consuming high-fat, low-carbohydrate and low-fat, high-carbohydrate isoenergetic diets. *The American journal of clinical nutrition* 77, 43–50. [PubMed: 12499321]

- Souza Pauli LS, Ropelle EC, de Souza CT, Cintra DE, da Silva AS, de Almeida Rodrigues B, de Moura LP, Marinho R, de Oliveira V, Katashima CK, Pauli JR & Ropelle ER. (2014). Exercise training decreases mitogen-activated protein kinase phosphatase-3 expression and suppresses hepatic gluconeogenesis in obese mice. *The Journal of physiology* 592, 1325–1340. [PubMed: 24396063]
- Tanida M, Gotoh H, Yamamoto N, Wang M, Kuda Y, Kurata Y, Mori M & Shibamoto T. (2015a). Hypothalamic Nesfatin-1 Stimulates Sympathetic Nerve Activity via Hypothalamic ERK Signaling. *Diabetes* 64, 3725–3736. [PubMed: 26310564]
- Tanida M, Shintani N & Hashimoto H. (2011). The melanocortin system is involved in regulating autonomic nerve activity through central pituitary adenylate cyclase-activating polypeptide. *Neurosci Res* 70, 55–61. [PubMed: 21291921]
- Tanida M, Yamamoto N, Morgan DA, Kurata Y, Shibamoto T & Rahmouni K. (2015b). Leptin receptor signaling in the hypothalamus regulates hepatic autonomic nerve activity via phosphatidylinositol 3-kinase and AMP-activated protein kinase. *J Neurosci* 35, 474–484. [PubMed: 25589743]
- Vernon G, Baranova A & Younossi ZM. (2011). Systematic review: the epidemiology and natural history of non-alcoholic fatty liver disease and non-alcoholic steatohepatitis in adults. *Aliment Pharmacol Ther* 34, 274–285. [PubMed: 21623852]
- Wilson CG, Tran JL, Erion DM, Vera NB, Febbraio M & Weiss EJ. (2016). Hepatocyte-Specific Disruption of CD36 Attenuates Fatty Liver and Improves Insulin Sensitivity in HFD-Fed Mice. *Endocrinology* 157, 570–585. [PubMed: 26650570]
- Wong CH, Jenne CN, Lee WY, Leger C & Kubes P. (2011). Functional innervation of hepatic iNKT cells is immunosuppressive following stroke. *Science* 334, 101–105. [PubMed: 21921158]
- Wu Q, Orregon AM, Tsang B, Doerge H, Feingold KR & Stahl A. (2006). FATP1 is an insulin-sensitive fatty acid transporter involved in diet-induced obesity. *Mol Cell Biol* 26, 3455–3467. [PubMed: 16611988]
- Young CN, Cao X, Guruju MR, Pierce JP, Morgan DA, Wang G, Iadecola C, Mark AL & Davisson RL. (2012). ER stress in the brain subfornical organ mediates angiotensin-dependent hypertension. *The Journal of clinical investigation* 122, 3960–3964. [PubMed: 23064361]
- Young CN, Morgan DA, Butler SD, Mark AL & Davisson RL. (2013). The brain subfornical organ mediates leptin-induced increases in renal sympathetic activity but not its metabolic effects. *Hypertension* 61, 737–744. [PubMed: 23357182]
- Young CN, Morgan DA, Butler SD, Rahmouni K, Gurley SB, Coffman TM, Mark AL & Davisson RL. (2015). Angiotensin type 1a receptors in the forebrain subfornical organ facilitate leptin-induced weight loss through brown adipose tissue thermogenesis. *Mol Metab* 4, 337–343. [PubMed: 25830096]

Key Points

- Non-alcoholic fatty liver disease, characterized in part by elevated liver triglycerides (i.e. hepatic steatosis), is a growing health problem.
- In this study, we found that hepatic steatosis is associated with robust hepatic sympathetic overactivity.
- Removal of hepatic sympathetic nerves reduced obesity-induced hepatic steatosis.
- Liver sympathetic innervation modulated hepatic lipid acquisition pathways during obesity.

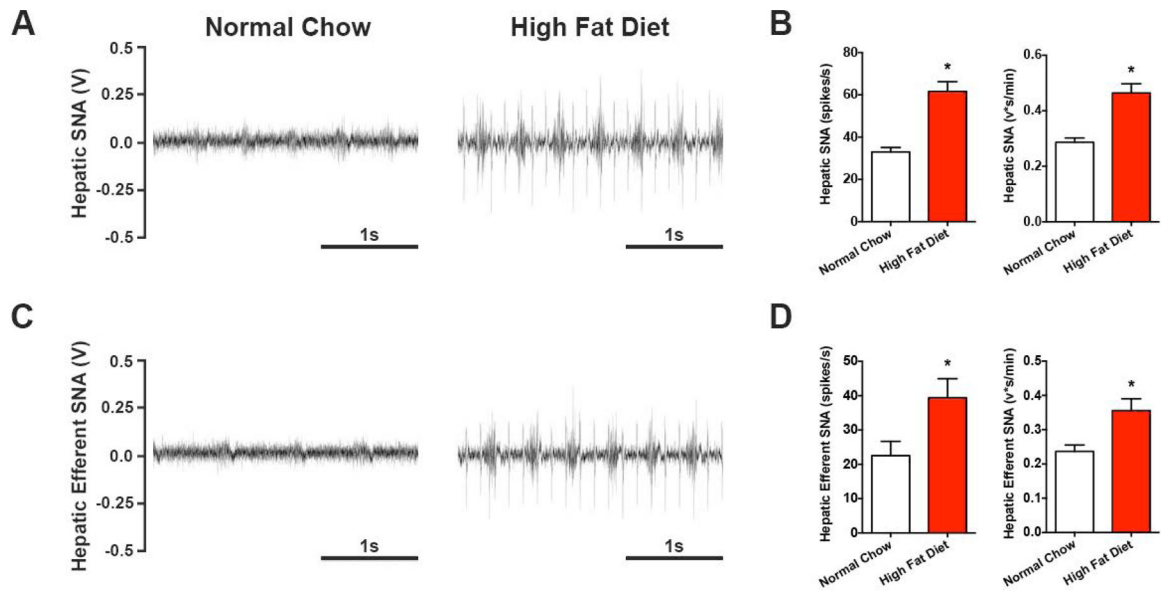


Figure 1. High fat diet feeding evokes robust elevations in hepatic SNA.

Direct multiunit recordings of hepatic SNA were obtained in high fat diet and normal chow controls. (A) Representative total hepatic SNA and (B) group summary data calculated as a frequency and integrated voltage. (C) Representative efferent hepatic SNA (nerve sectioned distal to recording electrode to eliminate afferent input) and (D) group summary data. (n=5–6). Student’s two-tailed unpaired t-test. *p<0.05 vs. normal chow.

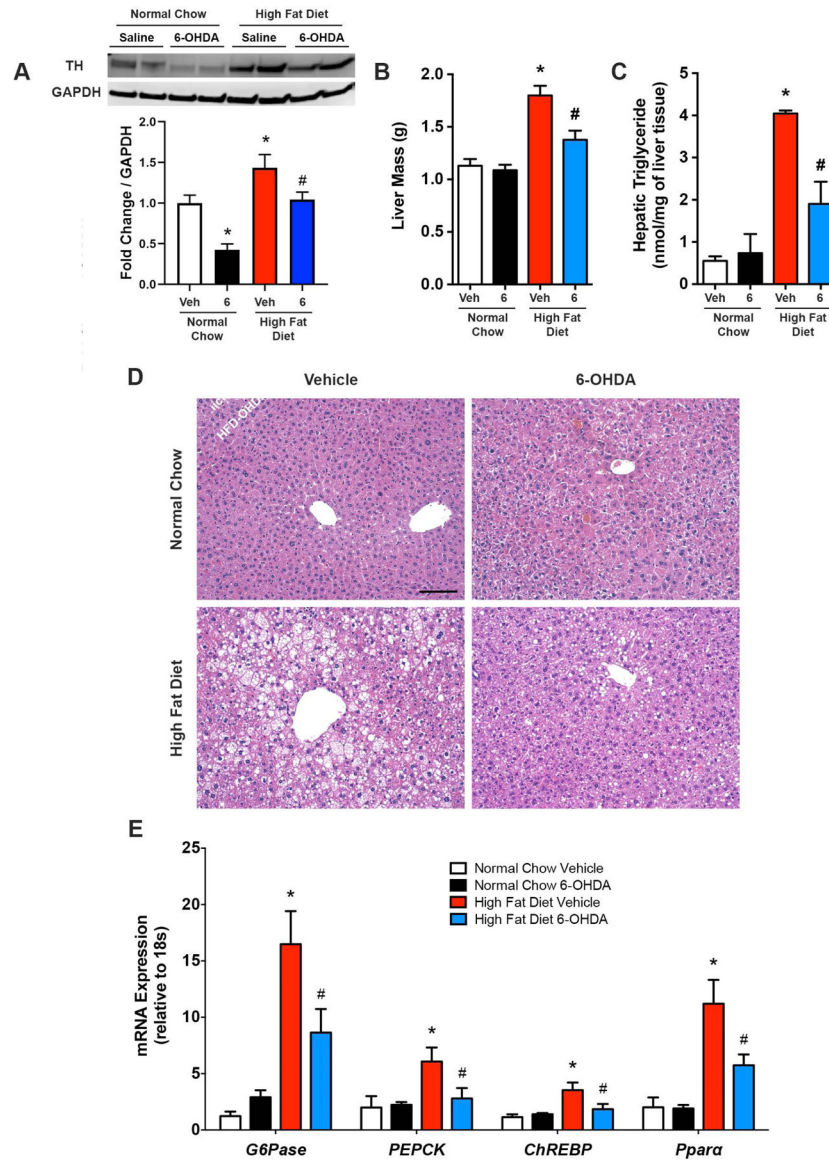


Figure 2. Pharmacological removal of sympathetic nerve activity reduces hepatic steatosis during diet-induced obesity.

6-hydroxydopamine (6) to ablate peripheral sympathetic nerves, or vehicle control (Veh), was administered (i.p.) once in high fat diet and normal chow fed mice and animals were sacrificed 3 days later. (A) Representative western blot and quantitative summary of liver tyrosine hydroxylase (TH) protein expression (n=4–8). (B) Liver mass (n=7–8). (C) Hepatic triglyceride content (n=4–7). (D) Representative liver hematoxylin and eosin staining. Scale bar=100 μ m. (E) mRNA expression of liver gluconeogenesis and de novo lipogenesis markers (n=7–8). Two-way ANOVA with Tukey's post-hoc test for all. * p <0.05 vs. normal chow, # p <0.05 vs. high fat diet vehicle.

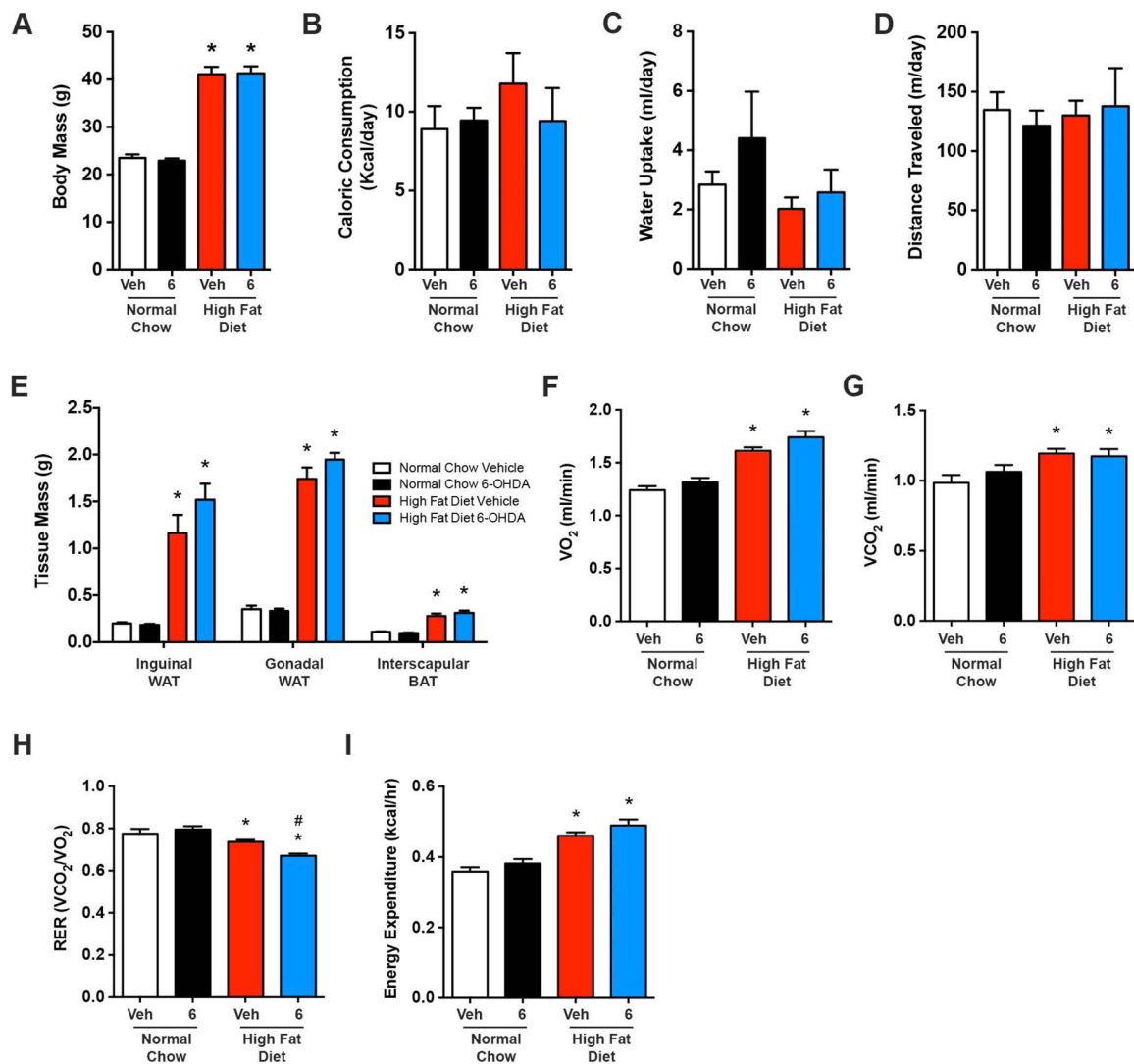


Figure 3. Pharmacological removal of sympathetic nerve activity does not influence body weight, food/water intake, locomotor activity, adiposity or energy expenditure.

(A) Body mass, (B) caloric consumption, (C) water intake, (D) locomotor activity, and (E) regional adipose tissue mass, as well as indirect calorimetry measurements of (F) oxygen consumption (VO₂), (G) carbon dioxide production (VCO₂), (H) respiratory exchange ratio (RER), and (I) energy expenditure following administration (i.p.) of 6-OHDA (6) to ablate peripheral sympathetic nerves, or vehicle control (Veh), in high fat diet and normal chow fed mice. n=7–8 for all. Two-way ANOVA with Tukey's post-hoc test for all. *p<0.05 vs. normal chow, #p<0.05 vs. high fat diet vehicle.

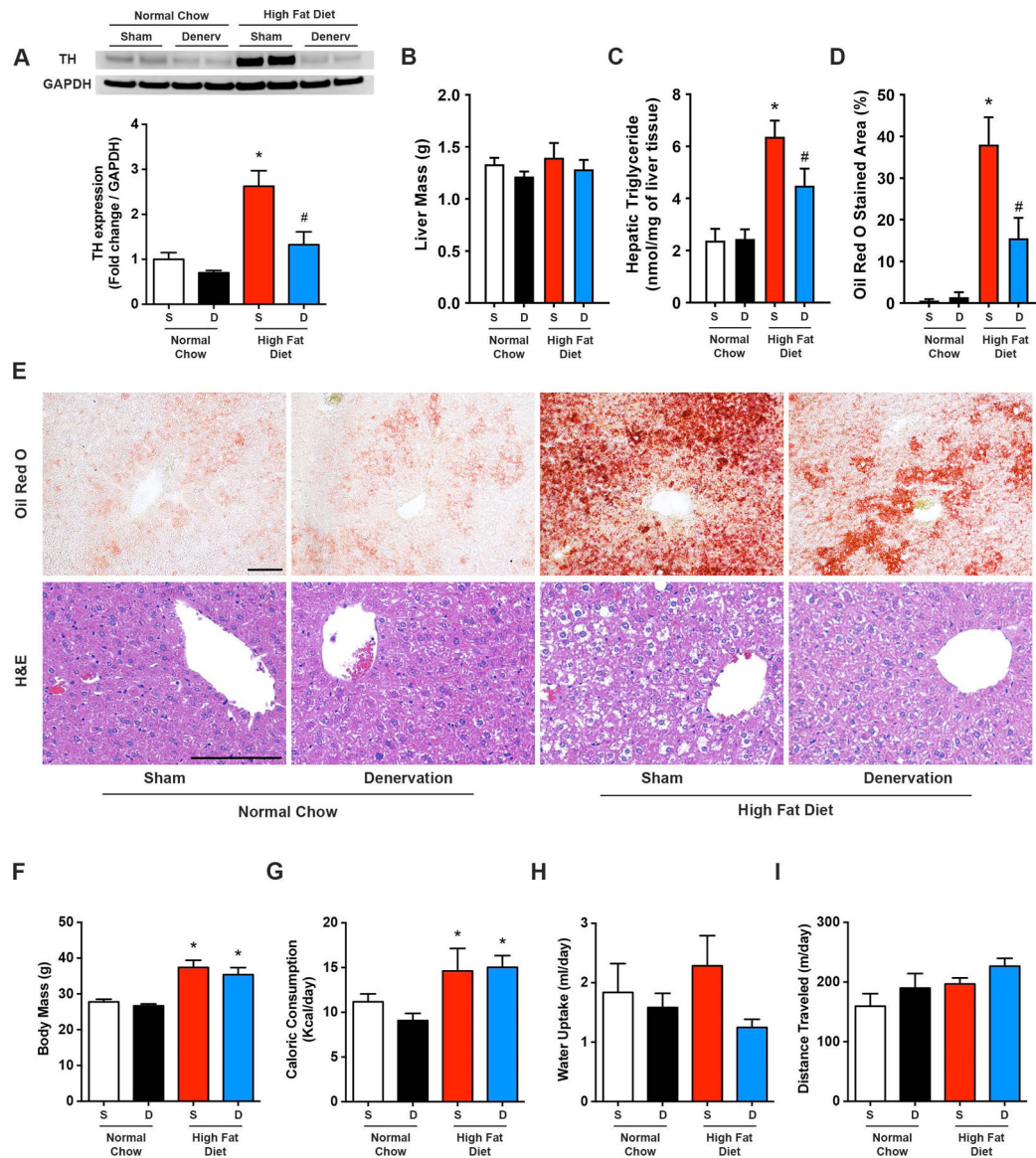


Figure 4. Hepatic denervation reduces diet-induced hepatic steatosis.

High fat diet and normal chow mice underwent selective hepatic denervation (D) or sham (S) surgery and were sacrificed 7 days later. (A) Representative western blot and quantitative summary of liver tyrosine hydroxylase (TH) protein expression (n=4–6). (B) Hepatic triglyceride content (n=4–8). (C) Liver Oil Red O stained area (n=3–4). (D) Representative Oil Red O and H&E liver staining. Scale bar=100 μ m. (E) Body mass, (F) caloric consumption, (G) water intake, and (H) daily locomotor activity (n=4–8). Two-way ANOVA with Tukey's post-hoc test for all. * p <0.05 vs. normal chow, # p <0.05 vs. high fat diet sham.

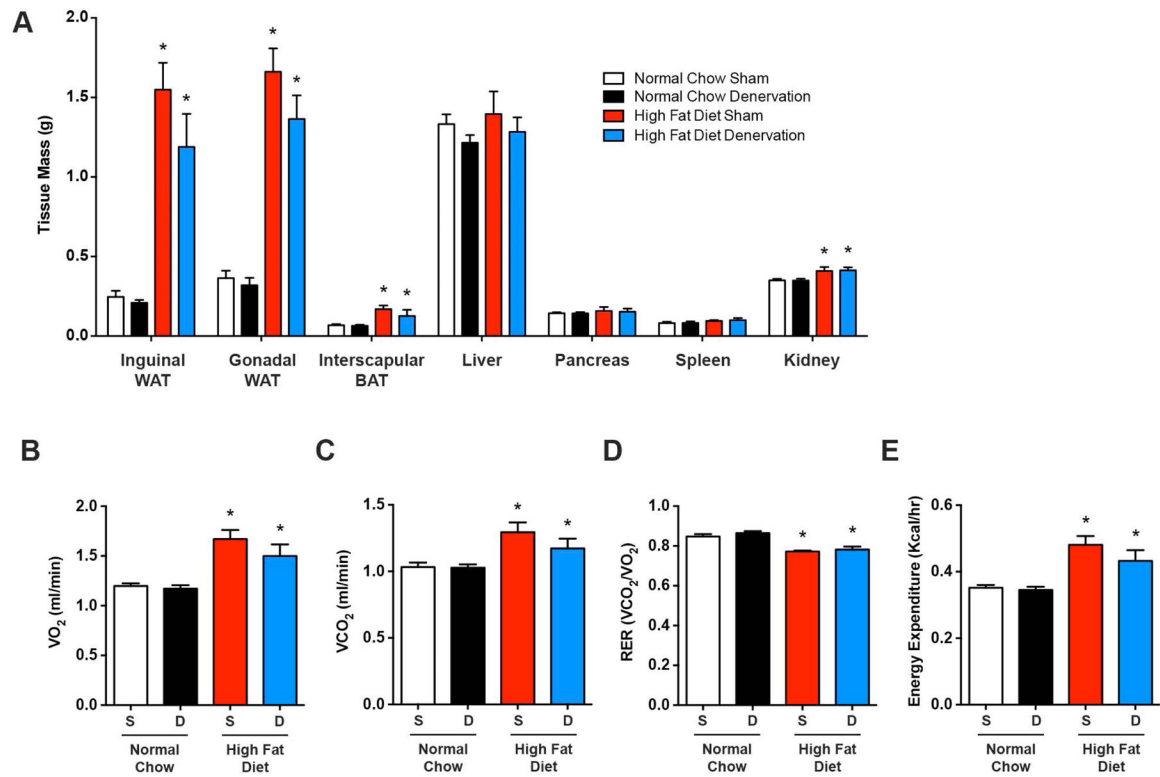


Figure 5. Short-term hepatic denervation does not affect adiposity, whole body energy utilization, and energy expenditure.

High fat diet and normal chow mice underwent selective hepatic denervation (D) or sham (S) surgery and were sacrificed 7 days later. (A) Masses of regional adipose tissue and organs that are innervated by the celiac and mesenteric ganglia (n=4–8). Indirect calorimetry measurements of (B) oxygen consumption (VO_2), (C) carbon dioxide production (VCO_2), (D) respiratory exchange ratio (RER), and (E) energy expenditure (n=4–8). Two-way ANOVA with Tukey's post-hoc test for all. *p<0.05 vs. normal chow.

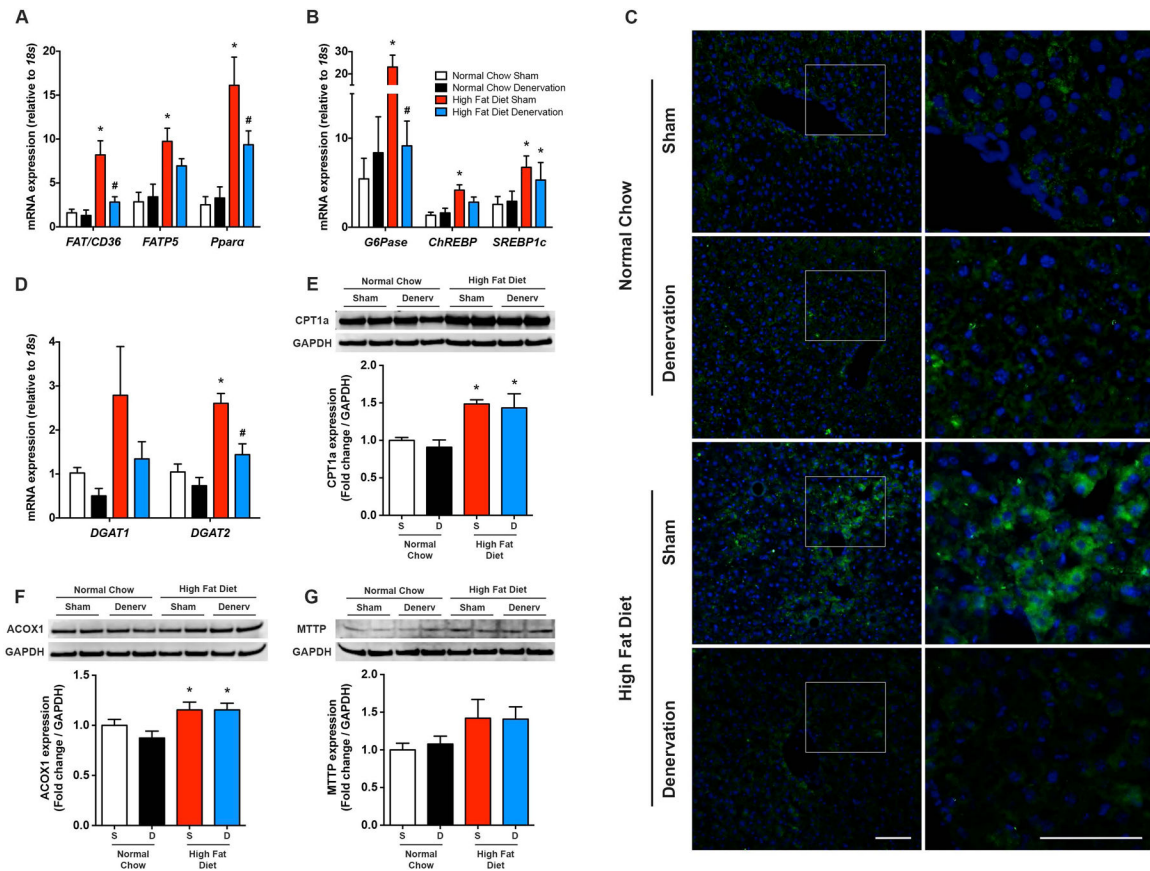


Figure 6. Hepatic denervation selectively decreases fatty acid uptake and de novo lipogenesis/gluconeogenesis pathways.

(A) Liver mRNA expression of fatty acid transporters and *Ppara* (n=4–7) and (B) de novo lipogenesis and gluconeogenesis markers (n=4–8) following sham (S) or hepatic denervation (D) surgery in normal chow control and high fat diet fed mice. (C) Representative immunohistochemistry for liver CD36 in sham and liver denervated animals. The right column represents a magnification of the white box in the corresponding image in the left column. Green; CD36, blue; DAPI, Scale bar=100 μ m. (D) Triacylglycerol synthesis markers (n=4–6). Representative western blot and quantitative summary of liver mitochondrial (E) and peroxisomal (F) β -oxidation markers, as well as (G) MTTP as a marker of VLDL export (n=4–6). Two-way ANOVA followed by Tukey's post-hoc test for all. *p<0.05 vs. normal chow, #p<0.05 vs. high fat diet sham.

Table 1.

Liver norepinephrine following 6-OHDA or phenol-based hepatic denervation

<i>Relative to respective vehicle</i>	Normal Chow Vehicle	Normal Chow 6-OHDA	High Fat Diet Vehicle	High Fat Diet 6-OHDA
Liver	1.00 ± 0.11	0.23 ± 0.10 *	1.00 ± 0.23	0.15 ± 0.03 *
<i>Absolute values</i>	5.21 ± 0.72	1.21 ± 0.55 *	4.23 ± 0.97	0.64 ± 0.12 *
<i>Relative to respective sham</i>	Normal Chow Sham	Normal Chow Denervation	High Fat Diet Sham	High Fat Diet Denervation
Liver	1.00 ± 0.22	0.44 ± 0.12 *	1.00 ± 0.25	0.33 ± 0.11 *
Spleen	1.00 ± 0.13	0.99 ± 0.13	1.00 ± 0.06	0.92 ± 0.11
Kidney	1.00 ± 0.03	0.90 ± 0.06	1.00 ± 0.05	1.01 ± 0.03
Pancreas	1.00 ± 0.15	0.75 ± 0.12	1.00 ± 0.07	0.88 ± 0.09
<i>Absolute values</i>	1.50 ± 0.44	0.66 ± 0.13 *	2.09 ± 1.56	1.18 ± 0.57
Liver	11.21 ± 2.06	13.94 ± 2.74	14.28 ± 4.92	22.73 ± 7.33
Spleen	14.31 ± 2.36	13.85 ± 2.94	10.00 ± 3.53	17.21 ± 5.00
Pancreas	10.03 ± 2.61	8.25 ± 2.44	10.36 ± 4.41	18.63 ± 6.69

Tissue norepinephrine measurements [absolute values (ng/mg protein) or relative to respective control group] three days following vehicle or 6-OHDA, as well as one week following sham or phenol-based hepatic denervation.

* p<0.05 vs. control within each diet group.

1.

Key Resources Table

Reagent and Resource	Source	Identifier
Antibodies		
Mouse anti-tyrosine hydroxylase	Santa Cruz	sc-25269
Rabbit anti-MTTP	Abcam	ab186446
Mouse anti-CPT1a	Abcam	ab128568
Rabbit anti-ACOX1	Abcam	ab184032
Rabbit anti-GAPDH	Abcam	ab181602
Rabbit anti-CD36	Novus Biologicals	NB400-144
Mouse anti-citrate synthase	Novus Biologicals	NBP2-43648
Goat anti-rabbit, HRP	Abcam	ab6721
Rabbit anti-mouse, HRP	Sigma-Aldrich	AP160P
Goat anti-rabbit, Alexa 488	Abcam	ab150077
Commercial Assays		
Triglyceride Assay Kit	Biovision	K622-100
Norepinephrine ELISA Kit	Labor Diagnostika Nord	BA E-5200
Other Chemicals		
6-hydroxydopamine (6-OHDA)	Sigma-Aldrich	162957
Oil Red O	Alfa Aesar	A12989
DAPI Mounting Medium	Vector Laboratories	H-1200
cDNA Conversion Kit	Quanta Bioscience	95048-100
SsoFast EvaGreen Supermix	Bio-Rad	1725202
qPCR Resources		
Primers	RefSeqs	qPCR primer sequences (5' → 3')
<i>18s</i>	NR_003278.3	F: GTAACCCGTTGAACCCATT R: CCATCCAATCGGTAGTAGCG
<i>G6Pase</i>	NM_008061.4	F: TGGTAGGCAACTGTTGTTGGTGC R: AGAATCCTGGGTCTCCTTGCCATT
<i>PEPCK</i>	NM_011044.2	F: GCCTGGATGAAGTTTGATGCCAA R: TTTGCTTCACTGAGGTGCCAGGA
<i>SREBP1c</i>	NM_001313979.1	F: GCAGCCACCATCTAGCCTG R: CAGCAGTGAGTCTGCCTTGAT
<i>ChREBP</i>	NM_021455.4	F: CCAGCCTCAAGGTGAGCAAA R: CATGTCCC GCATCTGGTCA
<i>Ppara</i>	NM_001113418.1	F: AAGAACCTGAGGAAGCCGTTCTGT R: GCAGCCACAAACAGGAAATGTCA
<i>FAT/CD36</i>	NM_001159555.1	F: ATTCCCTTGGCAACCAACCA R: CGTGGCCCGTTCTAATTCA
<i>FATP5</i>	NM_009512.2	F: GATGCTTTAGAGCGGCAAGC R: AACTTGGCCAACCCAGAAA
<i>DGAT1</i>	NM_010046	F: GTTTCCTCCAGGGTGGTAG R: GTTGGATCAGCCCCACTTGA

Reagent and Resource	Source	Identifier
<i>DGAT2</i>	NM_026384	F: CAGGTGCCGTCTTGGGTTAT R: CAGGAGGATATGCGCCAGAG

Author Manuscript

Author Manuscript

Author Manuscript

Author Manuscript